THE JOURNAL OF COMPARATIVE NEUROLOGY 470:400–408 (2004)

Immunoreactive TRPV-2 (VRL-1), a Capsaicin Receptor Homolog, in the Spinal Cord of the Rat

ROBIN D. LEWINTER,[1,2] KATE SKINNER,[1] DAVID JULIUS,[3] AND ALLAN I. BASBAUM[1,2]*
[1]Department of Anatomy, University of California, San Francisco, San Francisco, California 94143
[2]Department of Physiology, University of California, San Francisco, San Francisco, California 94143
[3]Department of Cellular and Molecular Pharmacology, University of California, San Francisco, San Francisco, California 94143

ABSTRACT

The vanilloid receptor-like 1 protein (VRL-1, also called TRPV2) is a member of the TRPV family of proteins and is a homolog of the capsaicin/vanilloid receptor (VR1, or TRPV1). Although VRL-1 does not bind capsaicin, like VR1 it is activated by noxious heat (>52°C). Unlike VR1, however, VRL-1 is primarily expressed by medium- and large-diameter primary afferents, which suggests that nociceptive processing is but one of the functions to which VRL-1 contributes. To provide information on the diverse spinal circuits that are engaged by these VRL-1-expressing primary afferents, we completed a detailed immunocytochemical map of VRL-1 in rat spinal cord, including light and electron microscopic analysis, and generated a more comprehensive neurochemical characterization of VRL-1-expressing primary afferents. Consistent with previous reports, we found that VRL-1 and VR1 are expressed in different dorsal root ganglion (DRG) cell bodies. Almost all VRL-1-expressing cells labeled for N52 (a marker of myelinated afferents), consistent with VRL-1 expression in Aδ and Aβ fibers. EM analysis of the DRG and dorsal roots confirmed this and revealed two categories of neurons based on the intensity of immunolabeling. The densest VRL-1 immunoreactivity in the spinal cord was found in lamina I, inner lamina II, and laminae III/IV. This is consistent with the expression of VRL-1 by myelinated nociceptors that target laminae I and IIi and in nonnociceptive Aβ fibers that target laminae III/IV. Dorsal rhizotomy reduced, but did not eliminate, the immunostaining in all dorsal horn laminae, which indicates that VRL-1 expression derives from both DRG cells and from neurons intrinsic to the brain or spinal cord. Spinal hemisection reduced immunostaining of the ipsilateral dorsal columns in segments rostral to the lesion and in the dorsal column nuclei, presumably from the loss of ascending Aβ afferents, but there was no change caudal to the lesion. Thus, supraspinal sources of dorsal horn VRL-1 immunoreactivity are likely not significant. Although we never observed VRL-1 immunostaining in cell bodies in the superficial dorsal horn, there was extensive labeling of motoneurons and ventral root efferents—in particular, in an extremely densely labeled population at the lumbosacral junction. Finally, many ependymal cells surrounding the central canal were intensely labeled. These results emphasize that VRL-1, in contrast to VR1, is present in a diverse population of neurons and undoubtedly contributes to numerous functions in addition to nociceptive processing. J. Comp. Neurol. 470:400–408, 2004.

Indexing terms: vanilloid receptor; nociception; dorsal horn; ultrastructure; TRP channel; immunocytochemistry

The VR1 subtype of the vanilloid receptor is the first member of the TRPV family. VR1 is a heat- and proton-gated nonselective cation channel that is responsive to the algogenic substance, capsaicin. VR1 is expressed by small-diameter neurons of the dorsal root ganglion (DRG) and mediates responses of nociceptive neurons to moderately noxious thermal stimuli (>43°C). The channel is essential for the development of hypersensitivity to thermal stimuli that follows tissue injury (Caterina et al., 1997; Davis et al., 2000; Chuang et al., 2001). This is presumed to result from the fact that protons and other components of the

Grant sponsor: National Institutes of Health; Grant number: DE 08973; NS21445; Grant number: NS14627.

*Correspondence to: Allan I. Basbaum, Department of Anatomy, University of California, San Francisco, Box 0452, San Francisco, CA 94143. E-mail: aib@phy.ucsf.edu

Received 20 June 2003; Revised 8 October 2003; accepted 31 October 2003
DOI 10.1002/cne.20024
Published online the week of February 2, 2004 in Wiley InterScience (www.interscience.wiley.com).

chemical milieu of tissue injury (such as nerve growth factor and bradykinin) significantly lower the thermal threshold for activation of the channel (Tominaga et al., 1998; Caterina and Julius, 1999; Chuang et al., 2001).

The extent to which VR1 underlies the normal response to noxious thermal stimuli and the relative contribution of other heat-sensitive channels is less clear. There is a dramatic reduction of heat sensitivity of DRG neurons that are cultured from mice with a disruption of the VR1 gene ($VR1^{-/-}$), but a small yet significant percentage showed large heat-evoked currents at high stimulus temperatures (>55°) (Caterina et al., 2000). These results are consistent with VR1 mediating responses to moderate painful temperatures. Recordings from a skin-nerve preparation of $VR1^{-/-}$ mice also revealed a significant decrease in the number of C fibers that responded to heat (peak temperature, 47°C) and those that did respond had a much reduced response magnitude. Finally, electrophysiological recordings of wide dynamic range neurons in lamina V of $VR1^{-/-}$ mice showed no response to stimuli at or below 49°C. Although higher temperatures were not studied in the electrophysiological studies, parallel studies of noxious heat-induced Fos expression in the VR1 mutant mice suggest that dorsal horn neurons can process higher temperatures. Thus, in wildtype mice a noxious (49°C) stimulus induced dense Fos staining in laminae I, II, and V. This was reduced, but not eliminated, in the mutant mice; significant residual Fos expression persisted in laminae I and II (Caterina et al., 2000). Taken together, these data strongly suggest that other heat-sensitive channels contribute to the transmission and ultimate perception of high-intensity noxious thermal stimuli.

One candidate is the TRPV2 channel, originally named the vanilloid receptor-like protein (VRL-1), which has ~50% sequence identity with VR1. The cloned VRL-1 protein does not respond to capsaicin, protons, or moderate heat. Rather, it is activated at high temperatures (>52°C) (Caterina, 1999; Ahluwalia et al., 2002). Initial studies showed that VRL-1 immunoreactivity is concentrated in a subset of medium- to large-diameter DRG neurons that do not express VR1 (Caterina, 1999; Ahluwalia et al., 2002). Recently, Ma (2001) and Ahluwalia et al. (2002) confirmed those results in the DRG, and Ichikawa and Sugimoto (2001) found a similar distribution of VRL-1 immunoreactivity (VRL-1-IR) in the trigeminal nucleus. VRL-1-IR neurons in the trigeminal ganglion innervate molar tooth pulp, afferents which are believed to be exclusively nociceptive (Ichikawa and Sugimoto, 2001). In addition, recent electrophysiological studies have shown that the native high-threshold heat (>52°) responses in cultured DRG neurons exhibit similar biophysical and pharmacological properties to those of heterologously expressed VRL-1 channels (Ahluwalia et al., 2002). Taken together, these observations suggest that VRL-1 is a marker of capsaicin-insensitive Aδ heat nociceptors. Based on the properties of VRL-1, we have suggested that VR1 and VRL-1 provide thermal sensitivity across a broad range of noxious temperatures, with VR1 sensitive to moderate temperatures and VRL-1 to more intense heat. In fact, when VR1 and VRL-1 are coexpressed in oocytes, a bimodal heat-evoked current is observed, indicating that these receptors can account for medium- and high-threshold thermosensation (Caterina et al., 1999). Whether or not VRL-1 mediates high-intensity heat pain responses in vivo awaits study of mice with a deletion of the VRL-1 gene.

Despite the emphasis on the contribution to the transmission of noxious heat messages, the presence of VRL-1 in relatively large DRG neurons suggests that its functional contribution is more complicated. In the present study, we used light and electron microscopic immunohistochemical approaches to extend our analysis. We concentrated on the pattern of expression in the spinal cord and on the neurochemical characterization of the populations of DRG neurons that express VRL-1.

MATERIALS AND METHODS

Experimental animals and procedures

All experiments were reviewed and approved by the Institutional Care and Animal Use Committee at the University of California San Francisco. Experiments were performed on male Sprague Dawley rats (Bantin and Kingman, Fremont, CA), weighing 250–300 g. Surgical procedures were performed under sodium pentobarbital anesthesia (50 mg/kg i.p.). To deafferent the spinal cord, we performed a laminectomy over the cervical enlargement and transected the C5-T1 dorsal roots with fine surgical scissors. To unilaterally transect ascending and descending pathways in the spinal cord, we used jeweler's forceps to hemisect the spinal cord at the level of T2. To transect the sciatic nerve, we made a small skin incision over the thigh and exposed the nerve by blunt dissection of the biceps femoralis. The nerve was then tightly ligated with 9-0 silk suture, just distal to the sciatic notch. The animals were euthanized 1 week following each procedure.

Light microscopic immunocytochemistry

Rats were deeply anesthetized with sodium pentobarbital (100 mg/kg, i.p.) and perfused intracardially with 50 ml of 0.1 M phosphate-buffered saline (PBS) followed by 500 ml of 10% formalin in 0.1 M phosphate buffer (PB), pH 7.4. The spinal cord and dorsal root ganglia were removed, postfixed in the same fixative for 4 hours, and cryoprotected overnight in a solution of 30% sucrose in 0.1 M PB. For immunostaining, we cut 30-μ spinal cord sections (L2–L6) on a freezing microtome. DRG were cut at 10 μm on a cryostat. Tissue sections were incubated for 60 minutes at room temperature in a blocking solution of 3% normal goat serum in PBS with 0.3% Triton X-100 (NGST). The sections were then incubated overnight at 4°C in primary antiserum, diluted 1:20,000 or 1:25,000. The characteristics of the antiserum, which was directed against the C-terminus of the rat VRL-1 receptor, have been described previously (Caterina et al., 1999). Next, the sections were washed three times in 1% NGST and visualized using either immunofluorescence or immunoperoxidase methods. For immunofluorescence we incubated sections in indocarbocyanine Cy-3-conjugated goat antirabbit IgG (Jackson ImmunoResearch, West Grove, PA; 1:600) for 2 hours at room temperature. Double label studies, using a different fluorophore, were performed either with a guinea pig anti-VR1 (1:5,000), monoclonal N52 (1:1,000, Sigma, St. Louis, MO) or plant lectin IB-4 (1:100, Sigma). Immunostaining was performed with an avidin-biotin peroxidase method that uses a nickel-intensified diaminobenzidine (DAB) protocol with glucose oxidase (Llewellyn-Smith et al., 1993). Reacted sections were mounted on gelatin-coated slides, dried, and coverslipped

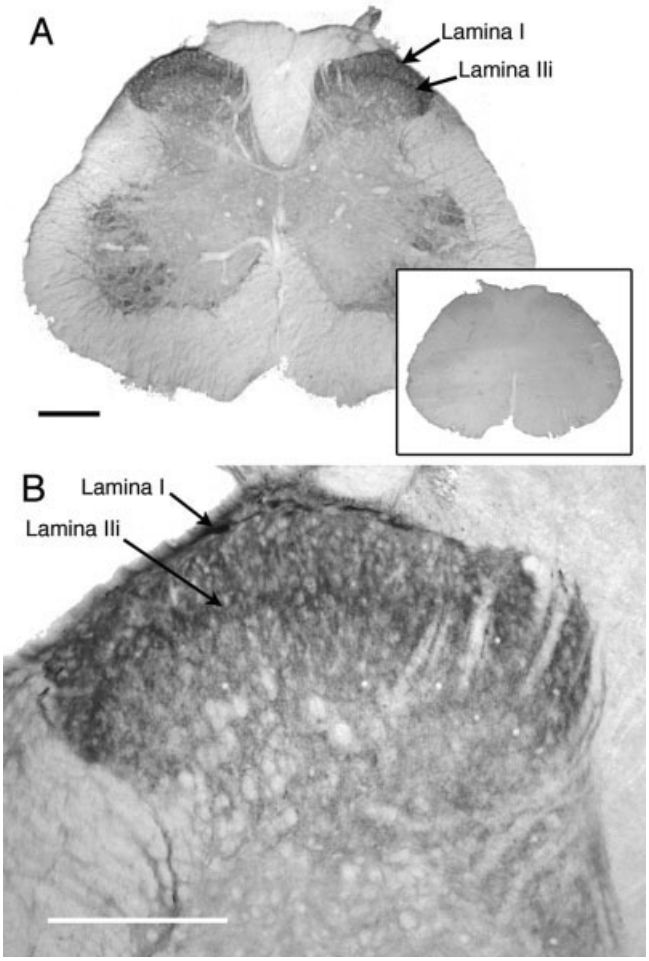

Fig. 1. This transverse section of the rat spinal cord (**A**) shows strong VRL-1 immunoreactivity throughout the superficial dorsal horn, most intensely in laminae I and IIi. Strong immunostaining is also seen in motor neurons and in ependymal cells surrounding the central canal. The higher magnification photomicrograph (**B**) shows the particularly concentrated immunostaining in lamina I and lamina IIi. The inset in A illustrates the loss of immunostaining when the primary antibody was preabsorbed with VRL-1 peptide. Scale bars = 300 μm.

with DPX (Electron Microscopy Science, Gibbstown, NJ). Sections were observed with a Nikon Eclipse fluorescence microscope. Images were scanned and processed in PhotoShop using a Spot RT Digital Camera (Diagnostic Instruments, Sterling Heights, MI). The specificity of the anti-VRL-1 antiserum was confirmed by the absence of staining of spinal cord tissue following preabsorption of the antibody with 10 μg/ml of the immunizing peptide (Fig. 1). To estimate the magnitude of rhizotomy-induced changes in immunoreactivity, we quantified the staining by densitometry as previously described (Abbadie et al., 1996). For this analysis, we captured five sections from the spinal cord of four deafferented rats using the Spot RT Digital camera and digitized the image with a computer-assisted image analysis program (NIH image). Because comparisons of immunostaining across animals is not reliable, we compared the density of the immunoreaction product on the deafferented and contralateral sides of the dorsal horn. Ratios of the density of immunostaining were calculated separately for laminae I and II and for laminae III and IV.

Electron microscopic immunocytochemistry

For electron microscopy, five adult rats were deeply anesthetized with pentobarbital and perfused through the heart first with Dulbecco's tissue culture medium (Sigma D-8900) and then 0.5% paraformaldehyde and 2% glutaraldehyde in PB. Lumbar DRGs were postfixed in the same solution for 4 hours and 50-μ transverse sections cut on a Vibratome. They were treated with 50% ethanol for 30 minutes to improve antibody penetration (Llewellyn-Smith and Minson, 1992), blocked in 5% NGS in Tris-PBS, pH 7.4 (TPBS), and then incubated in rabbit anti-VRL-1 antibody (1:20,000 or 1:25,000) in TPBS for 3 days. After washing in TPBS, sections were incubated in biotinylated goat antirabbit IgG (1:200), and then in HRP-conjugated Avidin (Sigma E2886, 1:1,500) for 1 day each. To localize the HRP, we used a nickel-intensified DAB protocol, which produces a flocculent reaction product, or a tetramethylbenzidine protocol, stabilized immediately by a cobalt-intensified DAB reaction, which produces a crystalline reaction product (Llewellyn-Smith et al., 1993). Sections were then osmicated and flat-embedded in Durcupan or Epon plastic resin. Selected regions were thin-sectioned and stained with uranyl acetate and lead citrate before being examined in a JEOL electron microscope. The electron microscope negatives were scanned and the digital images corrected for contrast and brightness with Adobe PhotoShop (Mountain View, CA), except where otherwise noted in the figure legends.

RESULTS

VRL-1 immunoreactivity (VRL-1-IR) in the spinal cord

VRL-1-IR is diffusely distributed throughout the spinal cord (Fig. 1A) at all segmental levels studied. The densest plexus of immunoreactive fine fibers and terminals is in lamina I and inner lamina II (IIi) (Fig. 1B). In most sections we detected a particularly dense focus of terminal staining in the midportion of lamina I. Less dense, but prominent VRL-1-IR is found in laminae III and IV, regions that receive input from relatively large-diameter nonnociceptive, Aβ primary afferents. Strong label was apparent in the intermediolateral (IML) cell column, which contains sympathetic preganglionic neurons. We also observed intense label in ependymal cells lining the central canal (Fig. 2A) as well as less strong labeling in relatively large neurons of the ventral horn (Fig. 2B,C). Many of the lightly stained ventral horn cells appear to be motoneurons, including neurons located in the sexually dimorphic nuclei (Schroder, 1980). In fact, we noted exceptionally dense staining in a subpopulation of ventral horn neurons at the lumbo-sacral junction (Fig. 2B). Based on their distribution, we hypothesize that these cells correspond to the sexually dimorphic neurons of the dorsolateral nucleus, which contains efferents that project to the external urethral sphincter and ischiocavernosus muscles (Schroder, 1980; McKenna and Nadelhaft, 1986).

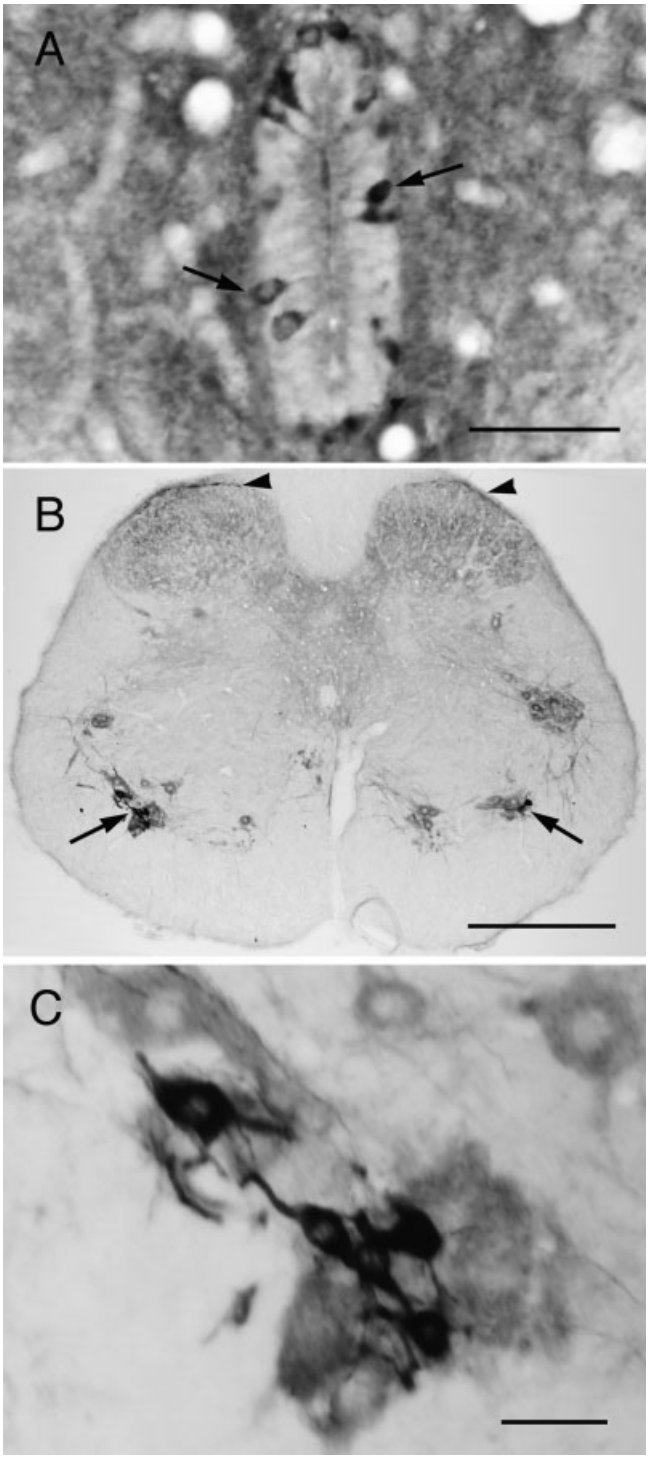

Fig. 2. These photomicrographs illustrate densely labeled cells adjacent to the central canal in a thick (50 μm) section of the lumbar spinal cord (**A**, arrows) and in a clustered population of presumed motoneurons in the ventral horn of the lumbosacral cord (shown at higher magnification in **C**). The latter are distributed among more lightly labeled motoneurons (**B**, arrows). The arrowheads in B point to the intense labeling in lamina I. Scale bars = 50 μm in A; 500 μm in B; 50 μm in C.

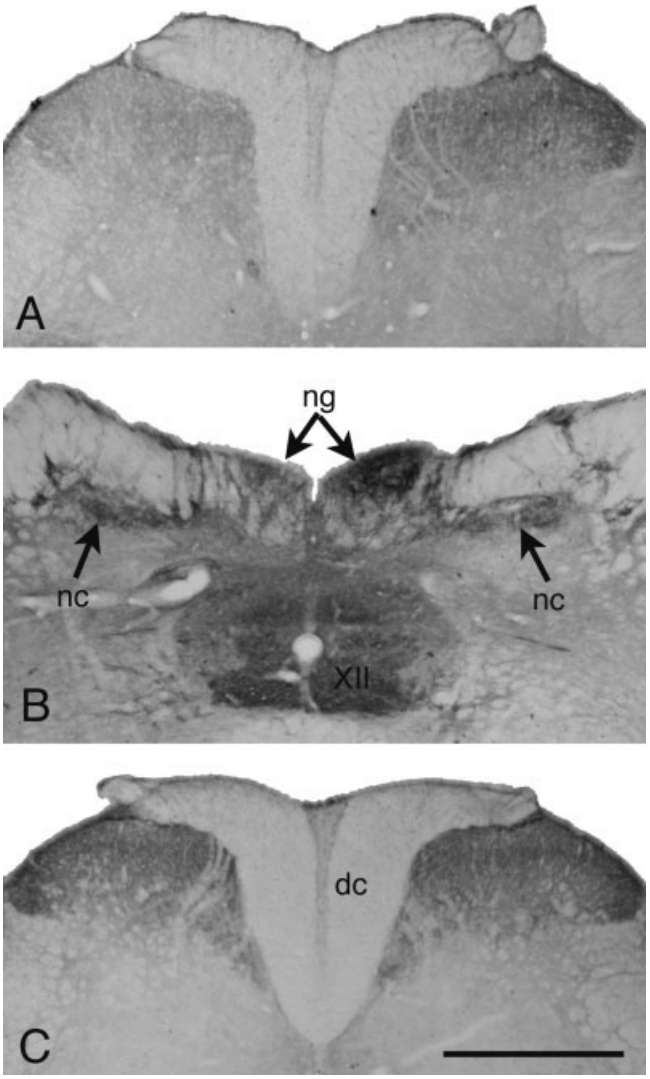

Fig. 3. Dorsal rhizotomy (**A**) reduces but does not eliminate immunostaining throughout the dorsal horn ipsilateral to the lesion. **B:** A caudal medulla section rostral to a hemisection performed at the level of the thoracic cord. There is significant reduction of the immunoreactivity in the nucleus gracilus ipsilateral to the hemisection. We found no change in the density of immunostaining caudal to the hemisection in **C**. For both rhizotomy and hemisection, the operated side is on the left. Scale bar = 500 μm. ng, nucleus gracilus, nc, nucleus cuneatus, dc, dorsal columns.

Origin of spinal cord VRL-1 immunoreactivity

As expected from the concentration of VRL-1 in primary afferents, we found that unilateral multiple rhizotomy of dorsal roots C5-T1 significantly decreased VRL-1-IR in the dorsal horn and in the nucleus proprius (laminae III and IV; Fig. 3). On average, rhizotomy decreased laminae I and II expression by 26% (±2%, n = 4) compared to the contralateral (intact side), and by 39% (±7%, n = 4) in laminae III and IV. The fact that the reduction occurred throughout the dorsal horn suggests that the immunoreactivity arises from large- and small-diameter primary

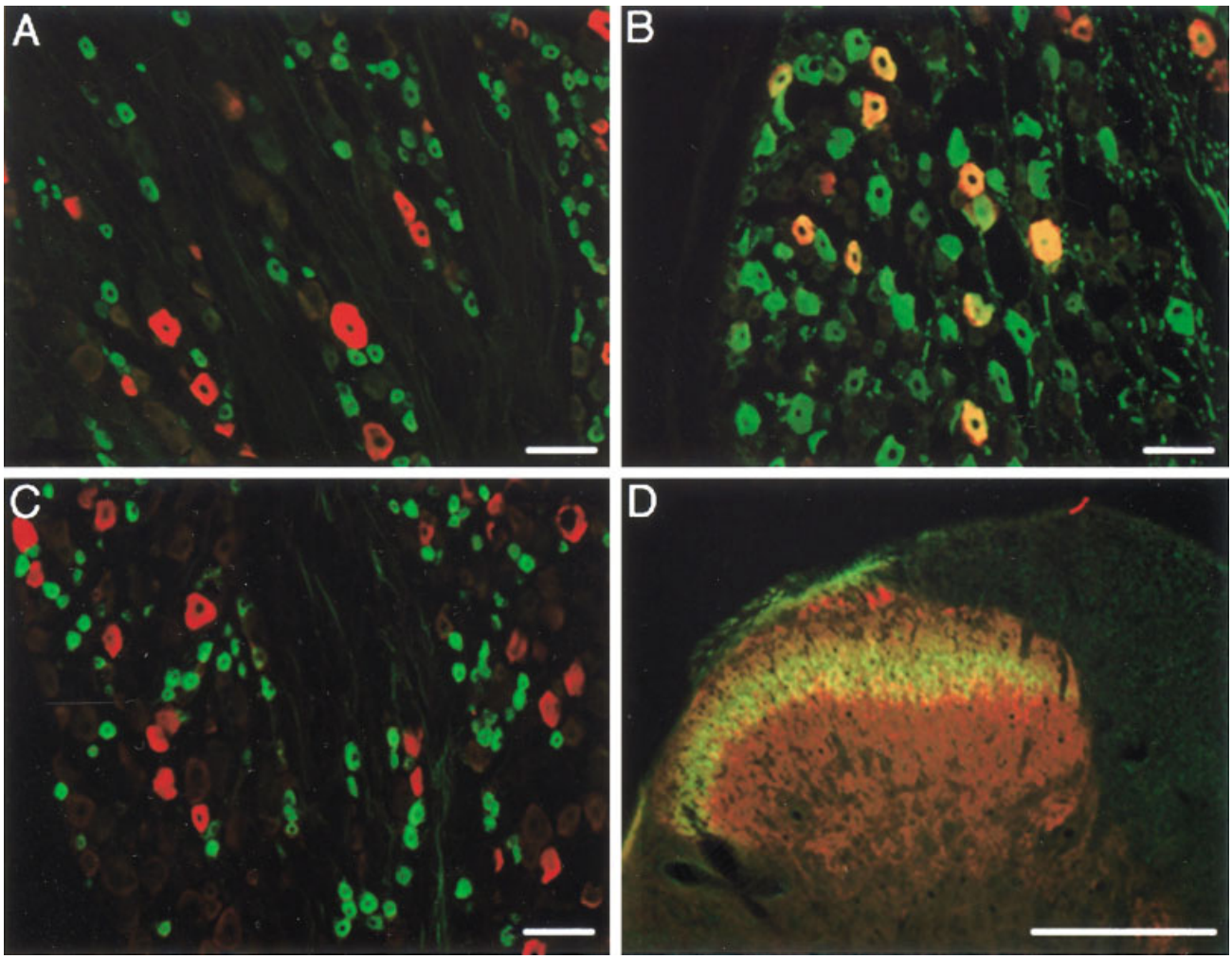

Fig. 4. To identify the neurochemistry of VRL-1 expressing DRG neurons, we performed double-label immunocytochemistry. VRL-1 (red) and VR1 (green) immunoreactivity does not colocalize (**A**), indicating that these TRP family members are expressed in different cell populations. All VRL-1-positive cells (red) colocalize with N52 (green) (**B**), indicating that VRL-1 is concentrated in myelinated afferents. Interestingly, although VRL-1 (red) does not colabel with neurons that bind the lectin IB4 (green) (**C**), there is extensive overlap of VRL-1- and IB4-positive terminals (yellow) in lamina IIi of the spinal cord (**D**). Note the intense labeling of VRL-1 in spinal cord lamina I (D). Scale bars = 100 μm in A–C; 500 μm in D.

afferents. On the other hand, even extensive rhizotomy never completely eliminated the spinal cord immunostaining. This suggests that a significant portion of the VRL-1-IR derives either from neurons intrinsic to the cord or from supraspinal sources.

To address the possible contribution of supraspinal sources, we performed a spinal cord hemisection of the thoracic cord to disrupt both ascending and descending pathways. We examined the tissue 1 week later. Rostral to the hemisection, in the cervical cord, we observed a profound decrease of VRL-1-IR in the nucleus gracilis and the fasciculus gracilis of the dorsal columns, ipsilateral to the lesion (Fig. 3B). We saw no change in expression in either the cuneate fasciculus or nucleus. Similar results were obtained in two animals. These findings are consistent with the presence of VRL-1 in large-diameter, Aβ primary afferent fibers that not only terminate in laminae III and IV of the dorsal horn, but also send collaterals via the dorsal columns to the medullary dorsal column nuclei. Caudal to the hemisection, at L4/L5 of the spinal cord, we found no change in immunoreactivity, either ipsilateral or contralateral to the lesion (Fig. 3C). We conclude that descending axons are not significant contributors to the VRL-1-IR distribution in the dorsal horn that survives dorsal rhizotomy. Rather, intrinsic sources are likely. Nevertheless, we have yet to observe immunostaining of cell bodies in the dorsal horn.

Defining the population of VRL-1 expressing neurons

We next addressed the heterogeneity of the primary afferent cell bodies that express VRL-1. As previously reported (Caterina, 1999; Ahluwalia et al., 2002) the majority of the immunoreactivity was concentrated in medium- to large-diameter DRG neurons (Fig. 4). Consistent with this result, we found that VRL-1-IR colocalizes

with N52, a marker of myelinated afferents (Fig. 4B). Further, as expected from the fact that few VRL-1-IR-positive cells contain substance P and only about 33% overlapped with calcitonin gene-related peptide (Caterina, 1999), we found no colocalization of VRL-1-IR with VR1 (Fig. 4A). This supports the conclusion that VRL-1 is a marker of capsaicin-insensitive cell bodies. Finally, VRL-1-IR did not colocalize with the lectin IB-4 (Fig. 4C), a marker of small-diameter fibers that project to lamina IIi. Interestingly, despite the segregation of VRL-1-IR- and IB-4-positive DRG neurons, we observed extensive overlap of the two markers in lamina IIi (Fig. 4D). This suggests that there is a convergence of unmyelinated (IB-4-expressing) and myelinated (VRL-1 expressing) nociceptors upon neurons in lamina IIi.

Electron microscopy

To further characterize the pattern of VRL-1 immunoreactivity, we examined the DRG and dorsal horn at the electron microscopic (EM) level. Plastic-embedded DRG tissue confirms that VRL-1 label is concentrated in medium to large cells (Fig. 5A). Electron microscopy of these same sections revealed three populations of DRG neurons (Fig. 5B): a densely stained population of large dorsal root ganglion neurons, a similarly sized population of lightly labeled neurons, and a diverse group that are clearly unlabeled. Label was found in scattered myelinated axons within the DRG, confirming its presence in larger diameter primary afferents (Fig. 6).

The EM analysis of the dorsal horn produced several surprising results. Of particular interest was the ultrastructure associated with the very dense patch of VRL-1 immunoreactivity in the mid-portion of lamina I. High-power light microscopic analysis suggested that this pattern of immunostaining resulted either from immunostaining of the entire periphery of labeled cell bodies in lamina 1 or corresponded to large numbers of immunoreactive axon terminals that surrounded unlabeled cell bodies (Fig. 7A). The EM analysis *in fact* showed that despite the dense concentration of VRL-1 in lamina I apparent at the light microscopic level, immunoreactivity at the ultrastructural level was remarkably sparse. This reflected the fact that VRL-1 label is patchily expressed, in exceptionally fine-diameter axonal profiles (<0.5 μm, Fig. 7B) and appears thinly distributed within axonal membranes. Labeled synapses were also difficult to identify (Fig. 7C). These findings, in combination with the light microscope double-label studies, suggest that the myelinated Aδ afferents that arborize in the superficial dorsal horn lose their myelin at a considerable distance from the terminals, where they appear as extremely fine unmyelinated fibers.

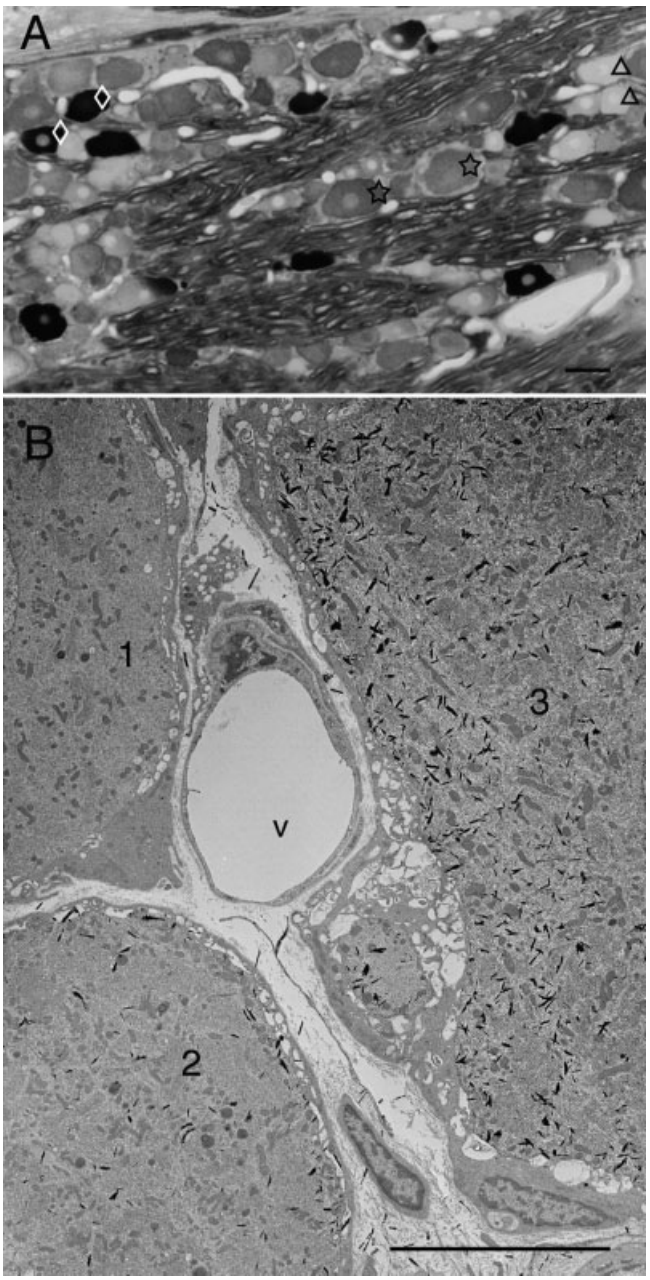

Fig. 5. Immunostaining of 2.0-μm semithin plastic-embedded DRGs (**A**) using TMB as chromogen reveals three populations of neurons: unlabeled (triangle), moderately labeled (star), and strongly labeled (diamond) cell bodies. Strongly labeled neurons are medium to large in size; both unlabeled and moderately labeled cells include large and small cells. EM analysis of these sections (**B**) confirmed this distribution of label (1, unlabeled; 2 moderately labeled; 3 strongly labeled; V capillary vessel). Scale bars = 100 μm in A; 10 μm in B.

DISCUSSION

The present immunohistochemical analysis of VRL-1 expression shows that this channel is widely distributed in the spinal cord. There is strong labeling in regions associated with nociceptive processing, particularly laminae I and IIi. Double-labeling immunocytochemistry shows that VRL-1 is associated with a complex subset of primary afferents, that likely include capsaicin-insensitive small myelinated Aδ neurons and larger Aβ myelinated mechanoreceptors. The former likely terminate in the superficial dorsal horn, including an intense concentration in lamina I, and the latter, we conclude, are the source of VRL-1 immunoreactivity in the neck of the dorsal horn (laminae III and IV), as well as in the posterior columns and dorsal column nuclei. The loss of immunoreactivity in the dorsal horn after dorsal rhizotomy taken together with the fact that sciatic nerve ligation resulted in a build-up of VRL-1-IR proximal to the ligation

Fig. 6. As expected from the colocalization of VRL-1 with N52, we observed dense label (crystalline reaction product) in myelinated axons within the DRG, consistent with the localization of VRL-1 in Aβ and Aδ afferents. This photomicrograph illustrates an intensely immunolabeled myelinated axon. Scale bar = 1.0 μm.

(data not shown) confirms that the protein is trafficked to both the central and peripheral terminals of DRG neurons.

Although we found almost complete overlap of VRL-1-IR positive neurons with N52, Ma (2001) reported only 46% colocalization of VRL-1-IR positive neurons with NF200 (N52) positive myelinated neurons. The difference in these results may be explained by the fact that different VRL-1 antibodies were used; the specificity of the two antibodies has also not been completely determined. Importantly, an absorption control performed with the antibody that we used abolished staining completely (Fig. 1, inset). The persistence of VRL-1 immunoreactivity after dorsal rhizotomy suggests that VRL-1 is localized to cell bodies intrinsic to the cord. Despite this conclusion, we never found labeled cell bodies in the dorsal horn. Conceivably, a different fixation method or intrathecal colchicine might reveal VRL-1 immunoreactivity in cell bodies in the spinal dorsal horn.

Of particular interest are the very strongly labeled cells that we found in the ventral horn of sections at the lumbosacral junction. Based on their location, we hypothesize that these neurons are part of the dorsolateral nucleus, which contains sexually dimorphic neurons that innervate the urethral sphincter and ischiocavernosus muscles (Schroder, 1980; Jordan et al., 1982; McKenna and Nadelhaft, 1986). Preliminary studies in our laboratory indicate that this label is indeed much more prominent in male than female rats. The function of VRL-1 in these neurons remains to be determined. An analysis of the function of VRL-1 at the neuromuscular junction in these sexually dimorphic systems will hopefully provide insights into the contribution of VRL-1 in this critical system.

In vitro data suggest that in the normal animal VRL-1 detects temperatures higher than those that activate VR1; the threshold for VRL-1 activation is ~52°C. Because the dense VRL-1-IR in laminae I and IIi arises predominantly from a myelinated afferent population, it appears that

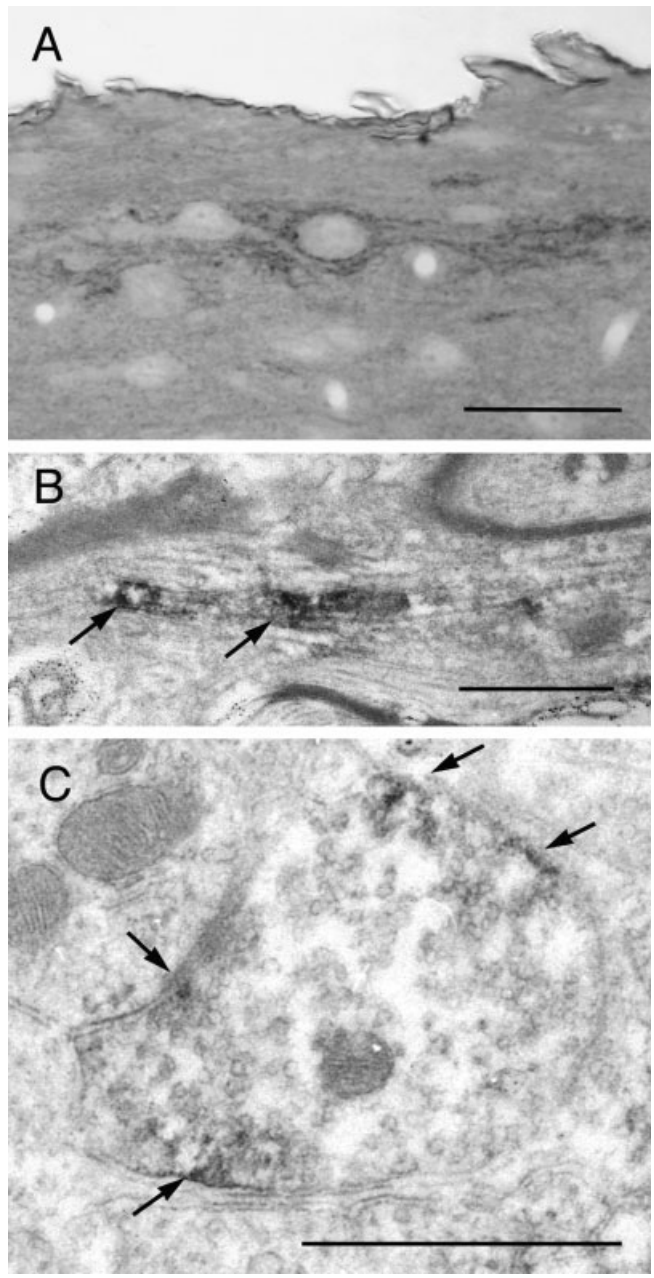

Fig. 7. This high-power light micrograph of VRL-1 immunoreactivity in a sagittal section of the lumbar dorsal horn (**A**, dorsal surface of the cord at top), shows a concentration of label in lamina I, which appears to outline large cell bodies and their processes. Electron microscopic analysis established that this pattern of immunoreactivity in lamina I derives from widely distributed, fine patchy DAB reaction product, in small unmyelinated axons (**B**) and small axon terminals (**C**) (arrows). Scale bars = 50 μm in A; 1.0 μm in B,C.

VRL-1 contributes to nociceptive processing via Aδ nociceptors. Interestingly, despite the density of labeling in the superficial dorsal horn, our EM analysis found few myelinated axons targeting this region. One possibility is these VRL-1 dorsal horn terminals arise from myelinated axons that lose their myelin far from the synaptic terminal and arborize as exceptionally fine unmyelinated

branches in lamina I (making them difficult to detect at the EM level). As such, these axons might correspond to the ultrafine axon terminals that Gobel et al. (1981) hypothesized arose from Aδ afferents.

Previous electrophysiological studies of the wide dynamic range (WDR) neurons in lamina V of VR1 mutant mice ($VR1^{-/-}$) showed that these neurons are largely unresponsive to thermal stimuli between 41° and 49° (Caterina et al., 2000), but there is a residual behavioral response to higher temperatures and noxious-heat-induced Fos expression is not completely lost in the dorsal horn of $VR1^{-/-}$ mice. We interpreted this result to mean that the behavior reflects summation of inputs over a large population of C fibers; the electrophysiological analysis of single afferents or dorsal horn neurons may thus be more indicative of transduction deficits rather than the behavioral consequences manifest by the integration of changes across large numbers of afferents. Specifically, a few afferents that continue to respond at temperatures near the VR1 threshold (presumably mediated by a different thermal detector, possibly VRL-1) may be sufficient to sustain behaviors at those temperatures. Note, however, that the residual thermal sensitivity is seen in both unmyelinated and myelinated axons, which suggests either that VRL-1 is present in both (as proposed by Ma, 2001), or, based on the present analysis, that as yet unidentified high threshold thermal transducers of C fibers are involved. Clearly, a better understanding of the contribution of VRL-1 to thermal and other processing is needed and will be revealed in mice with a deletion of this gene, as well as by analysis of mice in which both VR1 and VRL-1 have been deleted.

The concentration of VRL-1 immunoreactivity in primary afferents and in the superficial dorsal horn supports the hypothesized contribution of VRL-1 to nociception, but its widespread distribution emphasizes that VRL-1, in contrast to VR1, likely contributes to a variety of functions, in addition to thermosensation. For example, the presence of intensely immunoreactive ependymal cells surrounding the central canal raises the possibility that VRL-1 is involved in the transport of molecules from the CSF to parenchymal neurons and blood vessels in the spinal cord. Of particular interest are the intensely labeled cells in the ventral gray matter at the lumbosacral junction and in the intermediolateral cell column. Whether these cells are part of the sacral autonomic nucleus and ultimately affect bladder function and motility remains to be determined. In addition, axons of these strongly labeled cells may arborize to other laminae in the spinal cord and contribute to the intrinsic VRL-1-IR of the spinal cord. Interestingly, anatomical tracing studies of paraventricular neurons (PVNs) of the hypothalamus in the cat show projections to the IML and to Onuf's nucleus (which corresponds to the sexually dimorphic nuclei in the rat spinal cord) (Swanson and Kuypers, 1980; Holstege, 1987), areas which are VRL-1-IR-positive. The PVN also projects to the dorsal vagal nucleus and nucleus solitarius (Holstege, 1987), both of which label for VRL-1 (data not shown). Although PVN neurons do not immunostain for VRL-1, the correspondence of the PVN projections and the presence of VRL-1 immunoreactivity in the spinal cord suggests that the PVN may have a particular functional relationship with VRL-1 expressing neurons of the cord.

Consistent with the hypothesis that heat is not the only activator of VRL-1, Kanzaki et al. (1999) described a mouse homolog of VRL-1 with very different activation properties. The protein described by Kanzaki et al. (1999) translocates from intracellular pools to the plasma membrane upon stimulation with insulin-like growth factor-1 (IGF-1). Once translocated, this growth factor-regulated channel becomes an active calcium-permeable channel. It will be of interest to evaluate the effects of growth factors on the diverse VRL-1 populations in the spinal cord, as well as at the neuromuscular junction.

In summary, we have provided further evidence for a contribution of VRL-1 to thermoreception via myelinated nociceptors that terminate in the superficial dorsal horn. We also demonstrate that VRL-1 is strongly expressed in presumably nonnociceptive Aβ cells and in diverse neuron populations intrinsic to the spinal cord. Taken together, these data emphasize the complexity of VRL-1 and suggest that it has functions beyond thermal nociception.

ACKNOWLEDGMENT

The authors thank Dr. Michael Caterina for technical advice.

LITERATURE CITED

Abbadie C, Brown JL, Mantyh PW, Basbaum AI. 1996. Spinal cord substance P receptor immunoreactivity increases in both inflammatory and nerve injury models of persistent pain. Neuroscience 70:201–209.

Ahluwalia J, Rang H, Nagy I. 2002. The putative role of vanilloid receptor-like protein-1 in mediating high threshold noxious heat-sensitivity in rat cultured primary sensory neurons. Eur J Neurosci 16:1483–1489.

Caterina MJ. 1999. A capsaicin receptor homologue with a high threshold for noxious heat. Nature 398:436–441.

Caterina MJ, Julius D. 1999. Sense and specificity: a molecular identity for nociceptors. Curr Opin Neurobiol 9:525–530.

Caterina MJ, Schumacher MA, Tominaga M, Rosen TA, Levine JD, Julius D. 1997. The capsaicin receptor; a heat-activated ion channel in the pain pathway. Nature 389:816–824.

Caterina MJ, Leffler A, Malmberg AB, Martin WJ, Trafton J, Petersen-Zeitz KR, Koltzenburg M, Basbaum AI, Julius D. 2000. Impaired nociception and pain sensation in mice lacking the capsaicin receptor. Science 288:306–313.

Chuang HH, Prescott ED, Kong H, Shields S, Jordt SE, Basbaum AI, Chao MV, Julius D. 2001. Bradykinin and nerve growth factor release the capsaicin receptor from PtdIns(4,5)P2-mediated inhibition. Nature 411:957–962.

Davis JB, Gray J, Gunthorpe MJ, Hatcher JP, Davey PT, Overend P, Harries MH, Latcham J, Clapham C, Atkinson K, Hughes SA, Rance K, Grau E, Harper AJ, Pugh PL, Rogers DC, Bingham S, Randall A, Sheardown SA. 2000. Vanilloid receptor-1 is essential for inflammatory thermal hyperalgesia. Nature 405:183–187.

Gobel S, Falls WM, Humphrey E. 1981. Morphology and synaptic connections of ultrafine primary axons in lamina I of the spinal dorsal horn: candidates for the terminal axonal arbors of primary neurons with unmyelinated (c) axons. J Neurosci 1:1163–1179.

Holstege G. 1987. Some anatomical observations on the projections from the hypothalamus to brainstem and spinal cord: an HRP and autoradiographic tracing study in the cat. J Comp Neurol 260:98–126.

Ichikawa H, Sugimoto T. 2001. VR1-immunoreactive primary sensory neurons in the rat trigeminal ganglion. Brain Res 890:184–188.

Jordan CL, Breedlove, SM, Arnold AP. 1982. Sexual dimorphism and the influence of neonatal androgen in the dorsolateral motor nucleus of the rat lumbar spinal cord. Brain Res 249:309–314.

Kanzaki M, Zhang YQ, Mashima H, Li L, Shibata H, Kojima I. 1999. Translocation of a calcium-permeable cation channel induced by insulin-like growth factor-I. Nat Cell Biol 1:165–170.

Llewellyn-Smith KJ, Minson JB. 1992. Complete penetration of antibodies

into vibratome sections after glutaraldehyde fixation and ethanol treatment: light and electron microscopy for neuropeptides. J Histochem Cytochem 40:1741–1749.

Llewellyn-Smith IJ, Pilowsky P, Minson JB. 1993. The tungstate-stabilized tetramethylbenzidine reaction for light and electron microscopic immunocytochemistry and for revealing biocytin-filled neurons. J Neurosci Methods 46:27–40.

Ma QP. 2001. Vanilloid receptor homologue, VRL1, is expressed by both A- and C-fiber sensory neurons. Neuroreport 12:3693–3695.

McKenna KE, Nadelhaft I. 1986. The organization of the pudendal nerve in the male and female rat. J Comp Neurol 248:532–549.

Schroder HD. 1980. Organization of the motoneurons innervating the pelvic muscles of the male rat. J Comp Neurol 192:567–587.

Swanson LW, Kuypers HG. 1980. The paraventricular nucleus of the hypothalamus: cytoarchitectonic subdivisions and organization of projections to the pituitary, dorsal vagal complex, and spinal cord as demonstrated by retrograde fluorescence double-labeling methods. J Comp Neurol 194:555–570.

Tominaga M, Caterina MJ, Malmberg AB, Rosen TA, Gilbert H, Skinner K, Raumann BE, Basbaum AI, Julius D. 1998. The cloned capsaicin receptor integrates multiple pain-producing stimuli. Neuron 21: 531–543.